Global DFT-Based Reactivity Indicators: An Assessment of Theoretical Procedures in Zeolite Catalysis

ARTICLE *in* THE JOURNAL OF PHYSICAL CHEMISTRY C · JANUARY 2007

Impact Factor: 4.77 · DOI: 10.1021/jp0656227

4 AUTHORS, INCLUDING:

Karen Hemelsoet
Ghent University
56 PUBLICATIONS **874** CITATIONS
SEE PROFILE

Michel Waroquier
Ghent University
417 PUBLICATIONS **8,265** CITATIONS
SEE PROFILE

Global DFT-Based Reactivity Indicators: An Assessment of Theoretical Procedures in Zeolite Catalysis

Karen Hemelsoet,* David Lesthaeghe, Veronique Van Speybroeck, and Michel Waroquier*

Center for Molecular Modeling, Ghent University, Proeftuinstraat 86, B-9000 Ghent, Belgium

Received: August 30, 2006; In Final Form: November 23, 2006

The dependence of global reactivity descriptors on electronic structure method as well as basis set is investigated for typical reactions in zeolite catalysis. This research is especially focused on hard−hard interactions between small probe molecules (such as chloromethane, methanol, ethylene, and propene) and different zeolite clusters containing both oxygen and amine functionalities. The performance of novel hybrid metafunctionals (such as BMK and MPWB1K) on crucial reactivity predictors is assessed through comparison with both Hartree−Fock and B3-LYP results. For the complex bifunctional zeolite systems, we find accurate results using any of the DFT functionals, in conjunction with a basis set of at least double-ζ quality further augmented with both polarization and diffuse functions. Reactivity sequences, based on global softness differences as well as activation hardness values, are generally found to be independent of the level of theory whenever a DFT functional is used.

1. Introduction

Ab initio quantum mechanical calculations are nowadays widely used to rationalize all kinds of chemical problems. The standard wave function based Hartree−Fock (HF) method has proven successful, even though computational bond lengths and reaction barriers often overestimate experimental values. Although later refinements (called post-HF methods) lead to more accurate and reliable results, this is at the expense of computational efficiency, which becomes especially problematic when systems of medium or large molecular size are studied. Density functional theory (DFT), on the other hand, has gained a lot of attention over the years, based on an excellent cost-to-performance ratio.[1] Additionally, DFT provides important advantages as a conceptual theory,[2,3] enabling a precise definition for many commonly used chemical concepts such as electronegativity[4] and hardness.[5] These properties, currently referred to as DFT-based reactivity indicators, are defined as functional derivatives of the total electronic energy to the total number of electrons or the external potential.[2,6] In this paper, we will only focus on the so-called "global" indicators (as opposed to "local" indicators), which are used to describe the overall reactivity of a chemical system. These have been commonly applied to a broad variety of organic and inorganic chemical systems, discussing the reactive behavior of one single molecule or a set of related systems, occasionally even providing reactivity sequences for the latter (for a comprehensive review, see ref 3). Compared to traditional reaction rate theories such as transition state theory, calculations based on reactivity indicators are computationally less intensive (but in the same time less detailed) because all information is obtained through study of the reactants only.

Most studies in the field of DFT-based reactivity descriptors focus on their applicability and interpretative use, whereas little attention is generally given to the level of theory at which the indicators are computed. As a standard procedure, they are calculated by simply using the level as was used for the geometry optimization. The choice of basis set and the selection of a quantum mechanical Hamiltonian are nevertheless two essential points which can hardly be neglected, as the main advantage of the indicators is precisely their low computational cost. Furthermore, a strong level-of-theory dependence of the reactivity descriptors would almost certainly undermine their reliability. Relevant works investigating the performance of different theoretical procedures for describing reactivity-related properties are, however, rather scarce, and we will give a brief overview of the literature in the remainder of this paragraph. Most studies primarily assess the influence of the level of theory on local reactivity descriptors.[7] For the global indicators, however, only De Proft and Geerlings previously studied the effect of different theoretical methods on the electronegativity and hardness.[8] They concluded that all DFT methods perform better than the high-level coupled cluster method. A superior behavior was demonstrated for the B3-LYP and B3-PW91 functionals in particular. Additionally, Jalbout et al.[9] reported the excellent performance of the CBS-QB3 and G3B3 methods for a set of heteronuclear and homonuclear diatomic molecules. In an early work by Chattaraj and Schleyer, comparing HF and MP2 results, the effect of correlation was found to be important for the validity of the HSAB principle in the case of soft−soft interactions, whereas interactions involving the hard Ag^+ acid could be sufficiently described using the far less time-consuming HF level.[10] To our knowledge, all research presenting level-of-theory studies on global reactivity indicators is limited to this handful of papers.

For the practical computation of global reactivity descriptors, the finite difference method is by far the most popular. In this approach, the functional derivatives are written as appropriate combinations of the vertical ionization potential and electron affinity. These quantities are absolutely crucial in both experimental and computational chemistry and have consequently gained widespread attention. The computation of these energy differences is, however, not always straightforward: they are

* Authors to whom all correspondence should be addressed. E-mail: Karen.Hemelsoet@UGent.be (K.H.); Michel.Waroquier@UGent.be (M.W.).

10.1021/jp0656227 CCC: $37.00
Published on Web 01/26/2007

largely influenced by the incorporation of electron correlation in the calculation method and require the use of large basis sets, which becomes prohibitive for larger molecular systems.[11] Therefore, almost all studies so far have focused on testing a subset of two data sets developed by Pople and co-workers, denoted as G2−1[12] and G2−2.[13] These sets cover 148 neutral and 146 ionic species and contain extremely accurate experimental data. Whereas the G2−1 test set contains smaller molecules, the G2−2 test set also includes several larger systems such as substituted benzenes. For a recent overview on the electron affinities, we refer to the work of Schaefer and co-workers.[14] In addition to a detailed overview of experimental techniques, several DFT methods were also tested, demonstrating a satisfactory accuracy (within 0.2 eV) for larger molecules of the B3-LYP, BLYP, and BP86 functionals. This accuracy can be spectacularly improved when composite methods are used, e.g., G2 theory has average deviations of 0.06 eV for both ionization energies and electron affinities.[13] The computationally extremely demanding Wn procedures[15−17] show an absolute superior behavior, as W1 is characterized by a mean absolute deviation of 0.013 eV for the G2−1 set and 0.018 eV for the G2−2 set (minus 5 molecules, due to the size of the systems concerned).[16] These methods were, of course, specifically developed and parametrized on relatively small systems. Nevertheless, these studies emphasize how quantum mechanical methods have been developed beyond the level of just reproducing experimental data and are now capable of making accurate predictions where the experimental results are unknown or uncertain. It should also be noted that the electron affinity is typically only a fraction of the size of the ionization potential. Moreover, although every atom and molecule has an ionization potential, they need not necessarily have an electron affinity: there are quite some atomic and molecular negative ions that are simply not stable. Within this respect, density functional methods have been suggested to be fundamentally in error for the computation of anionic systems.[18] However, no convincing evidence was found to support this concern.[19] Moreover, a recent discussion has shown that DFT-based reactivity indicators, and the hardness in particular, can contribute to an improved understanding of this problem.[20]

In this paper, the influence of the level of theory on global DFT-based reactivity indicators is studied. More specifically, the effect of both basis set size and electronic structure method is thoroughly discussed. In order to probe the latter effect, HF (representing a wave function-based method) as well as three density-functional-based techniques are tested. The performance of the MPWB1K[21] and BMK functionals,[22] representing the latest class of hybrid metafunctionals, are assessed for the first time. These metafunctionals are primarily known for their successful description of kinetic properties. Even though the BMK functional is brand new, it has already shown promising results for various properties such as geometries and reaction barriers.[22,23] Overall, our main interest is to qualitatively investigate whether reactivity sequences remain unchanged when different levels of theory are used. This would also be the first time that large inorganic molecules such as zeolites are considered as a test set for an expanded assessment, as these molecules of considerable size are, quite logically, not included in the aforementioned G2−1 and G2−2 test sets.

As just mentioned, the present level-of-theory study on global reactivity indicators is performed on typical zeolite systems. Zeolites are microporous crystalline aluminosilicates, built from corner-sharing SiO_4 and AlO_4 tetrahedra. These solid-state catalysts portray a wide variety of properties and applications, due mainly to their shape-selectivity and Brönsted acid sites ≡Si−OH−Al≡, in combination with neighboring Lewis base ≡Si−O−Al≡ sites. The size of the zeolite clusters needed for an adequate description of the chemically active part, combined with the presence of different elements which all play a crucial role in defining the chemical properties, add to the challenge of describing these systems through global reactivity descriptors. This explains why the zeolite systems under study form an ideal test set for both absolute and relative values of these descriptors, outside the scope of G2−1 and G2−2. In addition to a traditional acidic zeolite cluster, we will also compare results with amine substituted zeolites,[24] allowing us to validate whether reactivity sequences in zeolites remain unaltered for different levels of theory. The appeal of nitrogen-substituted zeolites is mainly based on the minor change on the molecular level (substituting a single oxygen bridge by a N−H bridge), yet which leads to completely different reactivity profiles. By applying detailed theoretical calculations on reactions in both zeolite types using classical transition state theory, amine-based zeolites have shown to be catalytically more active than the conventional analogue with O linkages.[25,26] Therefore, these catalysts represent a new class of highly promising materials. In previous work, we specifically studied the interactions of chloromethane, methanol, ethylene, and propene with three zeolite model clusters (O, N1, and N2),[27] which are depicted in Figure 1. In addition to a kinetic description of these reactions, we also investigated their reactive behavior from the viewpoint of DFT-based reactivity descriptors.[28] Using both local and global descriptors, calculated at the B3-LYP/6-31G(d)//B3-LYP/6-31G(d) level of theory, we demonstrated that the interaction can be characterized as hard−hard, and that certain quantities are fully capable of predicting the reactivity sequences as a result of the amine-substitution. In general, the descriptors were found to provide valuable information on the catalytic abilities of the various clusters.[28]

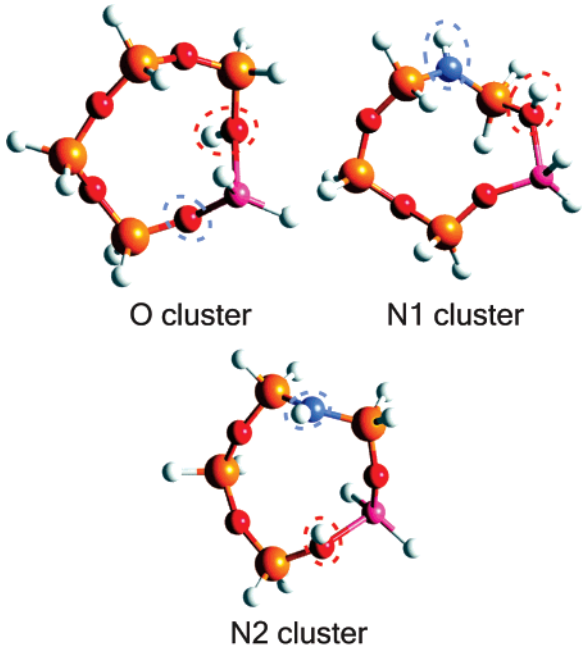

Figure 1. Optimized cluster geometries at B3-LYP/6-31G(d) level of theory, with acid site (red dotted line) and basic site (blue dotted line). For the O and N1 clusters both active sites are located on the same tetrahedron, whereas for the N2 cluster, the acid and base sites are further separated.

Summarizing, in this paper, we will validate whether the absolute values of global descriptors, which we previously calculated for some small molecules and a typical zeolite

containing only oxygen bridges on one specific level of theory, remain unchanged when different levels of theory are employed. We will investigate the low-cost HF method as well as three different DFT functionals, more precisely: B3-LYP, BMK, and MPWB1K. Although B3-LYP is the traditional functional of choice for calculations on zeolite systems, this is, to our knowledge, the first application of the hybrid metafunctionals MPWB1K and BMK in zeolite catalysis. In a next step, we will use the amine substituted zeolites to verify whether the choice in level of theory might influence reactivity sequences.

2. Global Reactivity Descriptors

The DFT-based reactivity indicators are defined as derivatives of the electronic energy $E[N,v(\mathbf{r})]$ with N the total number of electrons and $v(\mathrm{r})$ the external potential.[2,3,6] Global reactivity indicators provide information on the overall reactivity of a chemical system and are used to discuss reactivity sequences. The chemical potential (μ) equals the negative of the electronegativity, expressing the initial attraction toward electronic charge:

$$\mu = -\chi = \left(\frac{\partial E}{\partial N}\right)_v$$

The second derivative or hardness (η) measures the resistance to charge transfer, and the reciprocal is identified with the global softness (S)

$$\eta = \frac{1}{2S} = \left(\frac{\partial^2 E}{\partial^2 N}\right)_v$$

Using the finite difference approach, μ, η, and S can be computed from the vertical ionization potential (IP) and electron affinity (EA)

$$\mu = -\frac{\mathrm{IP} + \mathrm{EA}}{2}$$

$$\eta = \frac{\mathrm{IP} - \mathrm{EA}}{2}$$

$$S = \frac{1}{\mathrm{IP} - \mathrm{EA}}$$

The computation of these descriptors requires three single-point energy calculations. Nevertheless, as these calculations must be performed at a fixed geometry (the optimized geometry of the N-electron system), the computational effort in order to follow this procedure remains limited. The quantities are implemented in empirically well-known chemical principles. The hard soft acid base (HSAB) principle was originally discussed by Pearson[29] and states that a reaction between systems A and B will be favored when the global softness difference $\Delta S = S_A - S_B$ is minimal.[30] This rule was obtained through optimization of the covalent contribution of the interaction energy, consequently neglecting other effects such as polarization. According to the principle of maximal hardness (PMH),[31] molecules will rearrange themselves to achieve maximal hardness. Consequently, the transition state of a reaction should exhibit minimal hardness.[32] The activation hardness $\Delta\eta_{act} = \eta_{adsorbed\ reactant} - \eta_{transition\ state}$ describes hardness variations along the reaction path.[33] The smaller the activation hardness, the easier a reaction should occur.

3. Computational Methods

All calculations were performed using the Gaussian 03 software package.[34] The zeolite catalysts were simulated by a cluster built from 5 tetrahedral atoms (5T, T-atoms = Al or Si), which is capable of providing an adequate qualitative picture of chemical rearrangements that occur locally on the active site.[35,36] For the three zeolite clusters, the four probe molecules, as well as the adsorbed complexes, full geometry optimizations and frequency calculations using the hybrid B3-LYP functional[37,38] and 6-31G(d) basis set were performed as obtained in ref 25. The B3-LYP functional is known to provide accurate geometries within zeolite catalysis: Zygmunt et al. assessed the applicability of various readily available functionals for studying molecular adsorption in zeolite clusters and found that the B3-LYP functional gives intermolecular energies and vibrational frequencies similar to those obtained using MP2. Their final conclusion stated that the B3-LYP functional was the best choice for DFT treatment of zeolite clusters.[39] Nevertheless, we will also verify the suitability of the B3-LYP geometries by investigating the influence of the level of theory used for the geometry optimization. First, the performance of other functionals for geometry optimization, in particular BMK and MPWB1K, will be assessed. Second, we will upgrade the small basis set 6-31G(d) to 6-31+G(d,p), testing the influence of additional diffuse and polarization functions on the final geometry.

For the single-point energy calculations, four theoretical procedures were assessed. First of all, the standard Hartree−Fock (HF) method, in which correlation energy is completely neglected, was selected, due to the low computational cost. Note that the "DFT-based reactivity descriptors" are not rigorously defined within the HF scheme. However, we have used the finite difference approach to calculate these descriptors from the ionization potential and electron affinity obtained at the HF level. Furthermore, the popular B3-LYP hybrid functional[37,38] was applied. This functional is the standard choice to perform calculations within zeolite catalysis. In addition, two recently developed up-and-coming meta-gradient corrected functionals (BMK[22] and MPWB1K[21]) were also chosen, as their performance within the theory of conceptual DFT, as well as within zeolite catalysis, has not been investigated earlier.

Since the electron affinity values are very sensitive to the basis set,[40] as the addition of the electron entails a profound change in the spatial extent of the wave function of the anion, many Gaussian Pople basis sets were tested,[41] including 6-31G(d) (**1**), 6-31+G(d,p) (**2**), 6-311G(d,p) (**3**), 6-311+G(d,p) (**4**), 6-311++G(d,p) (**5**), and 6-311++G(3df,2p) (**6**). The performance of a selection of Dunning's correlation consistent basis sets,[42] cc-pVDZ (**7**), aug-cc-pVDZ (**8**), cc-pVTZ (**9**), and aug-cc-pVTZ (**10**) was also studied. The augmented basis sets **8** and **10** include one set of diffuse functions for each value of the angular momentum ℓ.

Additionally, for the smaller probe molecules (methanol, chloromethane, ethylene, and propene) high-level single-point energy calculations were performed, using the QCISD(T)[43] and CCSD(T)[44] post-HF methods in conjunction with the 6-311+G(d,p) and/or 6-311+G(3df,2p) basis sets. For these computations, the optimized B3-LYP/6-31G(d) geometries were used.

4. Results and Discussion

4.1. Comparison with Experiment: Small Probe Molecules. Resulting IP and EA values as well as their derived properties μ and η were calculated for four small probe molecules: chloromethane, methanol, ethylene, and propene. The calculated IP values were compared with available experimental data and mean absolute deviations (MADs) are reported in Table 1. The experimental IP values were obtained using

TABLE 1: Performance of Different Functional Methods[a]

	IP				μ and η			
	HF	B3-LYP	BMK	MPWB1K	HF	B3-LYP	BMK	MPWB1K
1. 6-31G(d)	1.43	0.25	0.25	0.25	1.62	1.21	1.31	1.28
2. 6-31+G(d,p)	1.36	0.11	0.14	0.16	0.72	0.21	0.34	0.31
3. 6-311G(d,p)	1.39	0.15	0.15	0.20	1.23	0.76	0.87	0.87
4. 6-311+G(d,p)	1.36	0.08	0.11	0.14	0.69	0.16	0.28	0.25
5. 6-311++G(d,p)	1.36	0.08	0.11	0.14	0.69	0.25	0.20	0.21
6. 6-311++G(3df,2p)	1.40	0.07	0.11	0.14	0.71	0.26	0.19	0.21
7. cc-pVDZ	1.42	0.20	0.20	0.21	1.43	0.97	1.10	1.07
8. aug-cc-pVDZ	1.38	0.09	0.12	0.15	0.70	0.31	0.20	0.16
9. cc-pVTZ	1.42	0.11	0.14	0.16	1.11	0.65	0.77	0.76
10. aug-cc-pVTZ	1.41	0.08	0.13	0.14	0.72	0.35	0.25	0.26
average values:								
over all basis sets	1.39	0.12	0.15	0.17	0.96	0.51	0.55	0.54
without diffuse functions	1.42	0.18	0.19	0.21	1.34	0.90	1.01	1.00
with diffuse functions	1.38	0.08	0.12	0.14	0.70	0.26	0.24	0.23

[a] Mean average deviations (MADs) in eV for the set of small probe molecules CH_3Cl, CH_3OH, C_2H_4, and C_3H_6. For the IPs the MADs are referred with respect to experiment, whereas for the global indicators μ and η the reference is the high level of theory QCISD(T)/6-311++G(3df,2p)//B3-LYP/6-31G(d).

photoelectron spectroscopy, amounting to 11.29 eV for chloromethane,[45] 10.96 eV for methanol,[46] 10.68 eV for ethylene,[47] and 9.91 eV for propene.[48]

From Table 1, it is immediately clear that the performance of the HF method is well below standard, showing deviations between 1.36 and 1.43 eV. In large contrast, the computed MAD values for the DFT functionals all indicate an excellent correlation with experiment, as the maximum MAD amounts to 0.25 eV, which corresponds to the smallest basis set 6-31G(d) taken into consideration. It is furthermore difficult to differentiate between the three DFT methods, as all of them succeed in an almost exact reproduction of the experimental data. The influence of the basis set is rather limited: the effect of adding extra polarization functions to a triple-ζ basis set (transition from basis set **5** to **6**) is, for instance, negligible. However, inclusion of diffuse functions leads to a substantial improvement of the results. This is a general observation, valid for both double- and triple-ζ basis sets. Furthermore, the Pople (**1**−**6**) and Dunning (**7**−**10**) basis set series perform very similarly, but because of the computational cost of the augmented basis sets, the latter series are not recommended for systems of considerable size. Overall, usage of 6-31G(d) and cc-pVDZ basis sets is discouraged.

As the global properties μ and η are not directly experimentally accessible and reliable experimental electron affinity data were not found, additional single-point energy calculations using the QCISD(T) and CCSD(T) levels, and using the B3-LYP/6-31G(d) optimized geometries, were performed (not included in Table 1). Among these, the QCISD(T)/6-311++G(3df,2p) level was chosen for benchmarking purposes as the MAD for the ionization potential with respect to the experimental values turned out to be the lowest (0.04 eV). MAD values for μ and η, resulting from comparison with the benchmark QCISD(T)/6-311++G(3df,2p) method, are given in Table 1. Closer inspection demonstrates how the three DFT functionals perform very similarly, whereas the HF MAD values are again substantially higher. All basis sets without diffuse functions perform poorly, irrespective of their double or triple-ζ character.

We conclude that for the computation of global descriptors, in the case of the four small probe molecules, accurate results can be obtained using either one of B3-LYP, BMK, or MPWB1K DFT functionals, in combination with a basis set of double-ζ or triple-ζ quality, augmented with both diffuse and polarization functions.

4.2. Reactivity Indicators: Purely Oxygen-Bridged Zeolites. Resulting IP, EA, μ and η values were calculated for the isolated, purely oxygen-bridged zeolite reactant (O cluster in Figure 1). Four electronic structure methods and nine basis sets were tested (in the remainder of the article the aug-cc-pVTZ basis set **10** is omitted, due to the large computational cost), and the results are reported in Table 2. Using the same extended set of various computational methods, global softness differences ΔS for the interactions between the O cluster and the small probe molecules were computed and consequently listed in Table 3. Finally, activation hardnesses $\Delta\eta_{act}$ were also calculated, using the optimized geometries of the adsorbed reactants and transition structures, and these values are given in Table 4.

4.2.1. Ionization Potential, Electron Affinity, Chemical Potential, and Hardness. The calculated IP values for this inorganic species (Table 2) show only a minor dependence on the level of theory, as they all lie in the narrow range between 9.35 and 9.90 eV. Inclusion of diffuse functions does not significantly alter the results. The EA values, on the other hand, vary more substantially, ranging from −0.19 to −2.81 eV. This effect is mostly attributed to the inclusion of diffuse functions, which are necessary for an accurate description of the more diffuse electron distribution of the anion state.

The influence of level of theory on the final geometry optimization was assessed for the purely oxygen-bridged zeolite cluster. The BMK/6-31G(d) and MPWB1K/6-31G(d) levels were used to assess the influence of a different functional and the B3-LYP/6-31+G(d,p) level was used to define the influence of a different basis set on the optimization. The sensitivity to geometry optimization is found to be extremely limited: Figure S1 in the Supporting Information depicts the global hardness of the zeolite catalyst which coincides for all levels of theory. The sole exception is formed by the low-cost HF single-point calculation on the MPWB1K optimized geometry, but the general trend is maintained nonetheless. Therefore, only the B3-LYP/6-31G(d) optimized geometries were retained in the remainder of this work.

The calculated μ varies between −3.40 and −4.69 eV, whereas η values range between 4.81 and 6.22 eV, indicating a relatively hard character of the investigated zeolite. The role of basis set is again restricted to the presence of diffuse functions, giving rise to a decrease of the hard character of the species with approximately 0.40 eV. We note that for all functionals under consideration, the 6-31+G(d,p), 6-311+G(d,p), 6-311++G(d,p), 6-311++G(3df,2p) and aug-cc-pVDZ results are extremely similar to one another. Based on these results, a double-ζ basis set, augmented with one set of diffuse

TABLE 2: Ionization Potentials, IP, Electron Affinities, EA, Chemical Potential, μ, and Global Hardness, η, for the Purely Oxygen-Bridged Zeolite[a]

	IP				EA			
	HF	B3-LYP	BMK	MPWB1K	HF	B3-LYP	BMK	MPWB1K
1. 6-31G(d)	9.65	9.37	9.77	9.78	−2.80	−1.35	−1.69	−1.59
2. 6-31+G(d,p)	9.68	9.48	9.86	9.86	−1.25	−0.41	−0.79	−0.67
3. 6-311G(d,p)	9.64	9.47	9.86	9.83	−2.27	−0.94	−1.32	−1.22
4. 6-311+G(d,p)	9.65	9.50	9.90	9.86	−1.20	−0.38	−0.76	−0.64
5. 6-311++G(d,p)	9.65	9.50	9.88	9.86	−1.03	−0.35	−0.68	−0.58
6. 6-311++G(3df,2p)	9.61	9.50	9.90	9.84	−0.96	−0.30	−0.61	−0.54
7. cc-pVDZ	9.62	9.35	9.74	9.75	−2.81	−1.33	−1.67	−1.58
8. aug-cc-pVDZ	9.57	9.43	9.77	9.77	−0.68	−0.19	−0.48	−0.39
9. cc-pVTZ	9.60	9.47	9.86	9.82	−2.36	−0.97	−1.32	−1.24
average values:								
over all basis sets	9.63	9.45	9.84	9.82	−1.70	−0.69	−1.04	−0.94
without diffuse functions	9.63	9.41	9.81	9.79	−2.56	−1.15	−1.50	−1.41
with diffuse functions	9.63	9.48	9.86	9.84	−1.02	−0.32	−0.66	−0.56

	μ				η			
	HF	B3-LYP	BMK	MPWB1K	HF	B3-LYP	BMK	MPWB1K
1. 6-31G(d)	−3.43	−4.01	−4.04	−4.09	6.22	5.36	5.73	5.68
2. 6-31+G(d,p)	−4.21	−4.54	−4.54	−4.60	5.47	4.95	5.32	5.26
3. 6-311G(d,p)	−3.69	−4.27	−4.27	−4.31	5.96	5.20	5.59	5.53
4. 6-311+G(d,p)	−4.22	−4.56	−4.57	−4.61	5.43	4.94	5.33	5.25
5. 6-311++G(d,p)	−4.31	−4.58	−4.60	−4.64	5.34	4.92	5.28	5.22
6. 6-311++G(3df,2p)	−4.33	−4.60	−4.65	−4.65	5.28	4.90	5.26	5.19
7. cc-pVDZ	−3.40	−4.01	−4.04	−4.09	6.21	5.34	5.70	5.66
8. aug-cc-pVDZ	−4.45	−4.62	−4.65	−4.69	5.13	4.81	5.12	5.08
9. cc-pVTZ	−3.63	−4.25	−4.27	−4.29	5.98	5.22	5.59	5.53
average values:								
over all basis sets	−3.96	−4.38	−4.40	−4.44	5.67	5.07	5.44	5.38
without diffuse functions	−3.54	−4.13	−4.15	−4.19	6.09	5.28	5.65	5.60
with diffuse functions	−4.30	−4.58	−4.60	−4.64	5.33	4.90	5.26	5.20

[a] All values are given in eV.

TABLE 3: ΔS Results in Absolute Values (au^{-1}) for the Reactions between the Probe Molecules and the Purely Oxygen-Bridged Zeolite

	zeolite O + CH_3Cl				zeolite O + CH_3OH			
	HF	B3-LYP	BMK	MPWB1K	HF	B3-LYP	BMK	MPWB1K
1. 6-31G(d)	0.321	0.677	0.556	0.557	0.399	0.741	0.635	0.641
2. 6-31+G(d,p)	0.274	0.594	0.467	0.478	0.185	0.546	0.406	0.414
3. 6-311G(d,p)	0.325	0.639	0.506	0.530	0.288	0.633	0.514	0.525
4. 6-311+G(d,p)	0.246	0.576	0.427	0.448	0.158	0.524	0.384	0.388
5. 6-311++G(d,p)	0.148	0.483	0.354	0.360	0.025	0.409	0.285	0.277
6. 6-311++G(3df,2p)	0.158	0.490	0.359	0.368	0.047	0.424	0.297	0.293
7. cc-pVDZ	0.303	0.640	0.534	0.537	0.295	0.639	0.544	0.547
8. aug-cc-pVDZ	0.226	0.533	0.417	0.410	0.097	0.454	0.337	0.322
9. cc-pVTZ	0.272	0.600	0.485	0.502	0.226	0.587	0.471	0.484
average values:								
over all basis sets	0.252	0.581	0.456	0.466	0.191	0.551	0.430	0.432
without diffuse functions	0.305	0.639	0.520	0.531	0.302	0.650	0.541	0.549
with diffuse functions	0.211	0.535	0.405	0.413	0.102	0.471	0.342	0.339

	zeolite O + C_2H_4				zeolite O + C_3H_6			
	HF	B3-LYP	BMK	MPWB1K	HF	B3-LYP	BMK	MPWB1K
1. 6-31G(d)	0.058	0.552	0.401	0.405	0.023	0.435	0.297	0.300
2. 6-31+G(d,p)	0.144	0.532	0.378	0.396	0.066	0.406	0.274	0.287
3. 6-311G(d,p)	0.095	0.567	0.403	0.412	0.017	0.448	0.301	0.308
4. 6-311+G(d,p)	0.166	0.543	0.385	0.405	0.125	0.411	0.276	0.289
5. 6-311++G(d,p)	0.011	0.392	0.408	0.419	0.139	0.168	0.056	0.031
6. 6-311++G(3df,2p)	0.003	0.401	0.413	0.429	0.059	0.178	0.062	0.041
7. cc-pVDZ	0.020	0.522	0.376	0.376	0.059	0.403	0.273	0.270
8. aug-cc-pVDZ	0.012	0.419	0.283	0.476	0.212	0.208	0.099	0.209
9. cc-pVTZ	0.043	0.521	0.360	0.375	0.032	0.404	0.261	0.272
average values:								
over all basis sets	0.061	0.494	0.379	0.410	0.081	0.340	0.211	0.223
without diffuse functions	0.054	0.540	0.385	0.392	0.033	0.422	0.283	0.288
with diffuse functions	0.067	0.458	0.373	0.425	0.120	0.274	0.153	0.171

functions and polarization functions (e.g., basis set **2**), seems sufficient for a reliable calculation of the global reactivity descriptors.

From a more interpretative point of view, μ can be applied to characterize the relative electrophilic or nucleophilic behavior of the involved molecules.[49] The chemical potentials for the

TABLE 4: $\Delta\eta_{act}$ Values (eV) for the Reactions between the Probe Molecules and the Purely Oxygen-Bridged Zeolite

	zeolite O + CH_3Cl				zeolite O + CH_3OH			
	HF	B3-LYP	BMK	MPWB1K	HF	B3-LYP	BMK	MPWB1K
1. 6-31G(d)	1.902	0.601	0.854	0.892	1.274	1.093	1.201	1.185
2. 6-31+G(d,p)	1.108	0.226	0.591	0.607	0.909	1.024	1.174	1.086
3. 6-311G(d,p)	2.155	0.501	0.731	0.784	1.075	1.085	1.232	1.159
4. 6-311+G(d,p)	1.044	0.387	0.591	0.600	0.871	1.006	1.159	1.041
5. 6-311++G(d,p)	0.949	0.347	0.528	0.526	0.888	0.948	1.054	0.988
6. 6-311++G(3df,2p)	1.507	0.311	0.607	0.514	0.890	0.955	1.063	0.983
7. cc-pVDZ	1.845	0.607	0.842	0.893	1.306	1.167	1.252	1.246
8. aug-cc-pVDZ	1.316	0.283	0.418	0.324	0.820	0.894	1.012	0.908
9. cc-pVTZ	2.319	0.419	0.798	0.829	1.267	1.165	1.294	1.249
average values:								
over all basis sets	1.572	0.409	0.662	0.663	1.033	1.037	1.160	1.094
without diffuse functions	2.055	0.532	0.806	0.850	1.230	1.127	1.245	1.210
with diffuse functions	1.185	0.311	0.547	0.514	0.876	0.965	1.092	1.001

	zeolite O + C_2H_4				zeolite O + C_3H_6			
	HF	B3-LYP	BMK	MPWB1K	HF	B3-LYP	BMK	MPWB1K
1. 6-31G(d)	1.616	1.092	1.275	1.304	2.151	1.452	1.722	1.730
2. 6-31+G(d,p)	1.089	0.852	1.015	1.024	1.526	1.509	1.436	1.408
3. 6-311G(d,p)	1.611	0.980	1.143	1.169	2.057	1.371	1.588	1.583
4. 6-311+G(d,p)	1.011	0.845	1.002	0.982	1.437	1.171	1.409	1.361
5. 6-311++G(d,p)	0.868	0.819	1.024	0.894	1.283	1.093	1.306	1.254
6. 6-311++G(3df,2p)	0.883	0.821	1.000	0.908	1.312	1.122	1.428	1.286
7. cc-pVDZ	1.531	1.096	1.255	1.282	2.058	1.454	1.678	1.697
8. aug-cc-pVDZ	1.285	0.743	0.964	0.795	1.206	1.049	1.368	1.184
9. cc-pVTZ	1.442	1.014	1.196	1.204	1.983	1.407	1.605	1.622
average values:								
over all basis sets	1.259	0.918	1.097	1.063	1.668	1.292	1.504	1.458
without diffuse functions	1.550	1.046	1.217	1.240	2.062	1.421	1.648	1.658
with diffuse functions	1.027	0.816	1.001	0.921	1.353	1.189	1.389	1.298

four probe molecules are tabulated in Table S2 of the Supporting Information. All Pople basis sets including diffuse functions succeed in a correct prediction of the stronger electrophilic behavior of the polar molecules (methanol and chloromethane) and a more nucleophilic behavior for the apolar molecules (ethene and propene). This is clearly illustrated in Figure 2, where the variation of the chemical potential depending on basis set size is depicted. As functional sensitivity was found to be small, only BMK results are included in Figure 2. The basis sets without diffuse functions, on the other hand, do not show a clear separation between molecules with polar and apolar character. Large deviations are clear for methanol in particular.

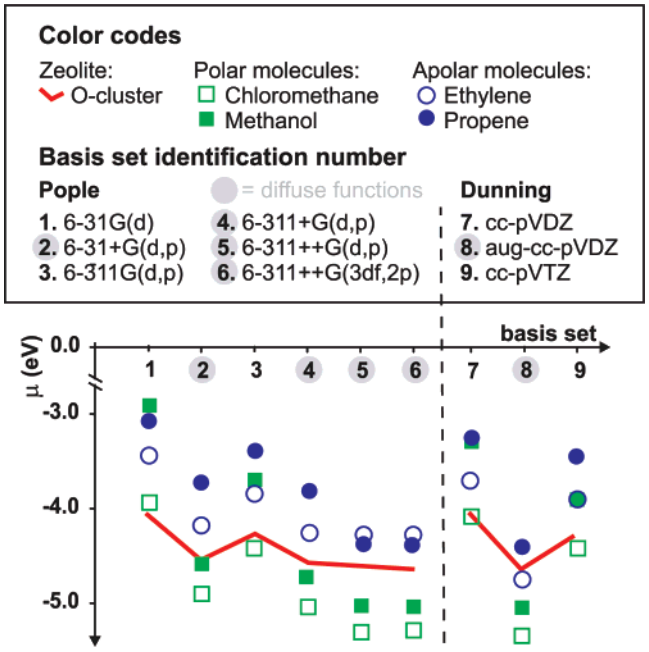

Figure 2. μ values for the O cluster (red line) and the four probe molecules chloromethane, methanol, ethylene and propene, calculated using the BMK functional (polar molecules: green; apolar molecules: blue).

4.2.2. Softness Differences. In Table 3, we list ΔS for the interaction between the four small probe molecules and the purely oxygen-bridged zeolite cluster. Large variations occur depending on both basis set and electronic structure method, but the overall predictions for ΔS are systematically larger for the two polar molecules compared to the apolar systems. Closer inspection of Table 3 reveals that the BMK and MPWB1K functionals predict almost identical values, whereas the HF predictions show large deviations from the DFT results. Concerning basis set dependence, the lack of diffuse functions will most often lead to higher ΔS values. At any rate, caution is absolutely necessary when applying the softness matching criterion to predict reaction preferences, as conclusions may depend on the applied level of theory. For sake of completeness, Table S1 of the Supporting Information tabulates the influence of the level of theory used for the geometry optimization on the average ΔS values. Yet again, this influence is negligible and our choice for B3-LYP/6-31G(d) geometries is warranted.

4.2.3. Activation Hardnesses. The $\Delta\eta_{act}$ values (Table 4) use information from the adsorbed reactants as well as from transition state structures. The smaller the $\Delta\eta_{act}$ value, the easier the reaction should proceed and the lower the reaction barrier should be. In ref 28, we compared $\Delta\eta_{act}$ values with energy barriers at 0 Kelvin (ΔE_0, Table 5; all properties were calculated using the B3-LYP/6-31G(d)//B3-LYP/6-31G(d) level of theory). Based on the ΔE_0 values, the following reactivity sequence corresponding to the interactions between the various small probe molecules and the purely oxygen-bridged cluster was obtained: propene < ethylene < chloromethane < methanol. No correlation exists between ΔE_0 and $\Delta\eta_{act}$, leading to the

TABLE 5: ΔE_0 Values (kJ/mol) for Chemisorption Reactions, ZPE Included, Taken from ref 28

	ΔE_0			
B3-LYP/6-31G(d)	CH_3Cl	CH_3OH	C_2H_4	C_3H_6
O	169.9	199.8	96.6	86.0
N1	220.3	165.8	141.0	117.6
N2	117.5	150.3	124.3	119.6

conclusion that the reactivity descriptor $\Delta\eta_{act}$ is inadequate in differentiating between the reactivities of the various probe molecules. The present study strongly confirms this conclusion: no correlation is obtained between the ΔE_0 and $\Delta\eta_{act}$ values, regardless of the level of theory used (see Table 4). We readily see that the overall $\Delta\eta_{act}$ value is smallest in the case of adsorption of chloromethane, while slight deviations can be noticed in the estimates predicted for methanol and ethylene. The largest values are found for propene. We note that for the current study the energy barriers were recalculated using the various levels of theory (included in Table S3 in the Supporting Information), but they do not differ qualitatively from the values at the B3-LYP/6-31G(d) level (displayed in Table 5). Finally, we report that the absolute values of HF differ substantially from the DFT results. The various $\Delta\eta_{act}$ predictions can again be classified in two categories, depending on the inclusion or exclusion of diffuse functions in the basis set.

4.3. Reactivity Sequences: Amine-Modified Zeolites. Comparison with kinetic data, such as ΔE_0 (Table 5), becomes more challenging when various zeolite clusters are compared. As in previous works of the authors, amine-substituted zeolite clusters (Figure 1) have been intensively investigated.[25,27] They form a suitable set of zeolite clusters to further validate the various rules on global reactivity descriptors. In particular, we will investigate whether the reactivity sequences between the three zeolite model clusters, as predicted in ref 28 using B3-LYP/6-31G(d), are maintained throughout the various levels of theory.

4.3.1. Hardness Sequence. In Tables S4 and S5 of the Supporting Information, the calculated IP and EA values as well as their derived global properties are given for the isolated amine-substituted zeolite models N1 and N2. It was earlier reported that all three investigated clusters are considered intermediately hard and that substitution of an oxygen by a nitrogen atom lowers the hardness, increasing the reactivity of the amine-modified cluster.[28] These conclusions were based on B3-LYP/6-31G(d) results, we now demonstrate that the hardness sequence $\eta(O) > \eta(N2) > \eta(N1)$ is retained for all investigated levels. The average difference between the $\eta(O)$ and $\eta(N2)$ values is 0.14 eV, whereas the average difference between the amine-substituted hardness values N2 and N1 is much smaller (0.07 eV). The reported hardness sequence indicates that substitution of an oxygen by a nitrogen atom lowers the hardness, increasing the reactivity of the amine-modified cluster.

4.3.2. Softness Differences. Global softness differences are calculated for the interactions between the three zeolite clusters and the probe molecules. Chloromethane and ethylene were chosen as the case study polar and apolar system, respectively. It was previously observed, using the B3-LYP/6-31G(d) level of theory, that for the interactions with the polar molecules, the HSAB principle fails due to a lack of any correlation between ΔS and ΔE_0.[28] This failure illustrates the limitations of the HSAB principle, where polarization effects are only partially included. For the apolar molecules however, the HSAB was shown to be successful.[28] In Figures 3 and 4 results for chloromethane and ethylene are illustrated. The following conclusions can be made.

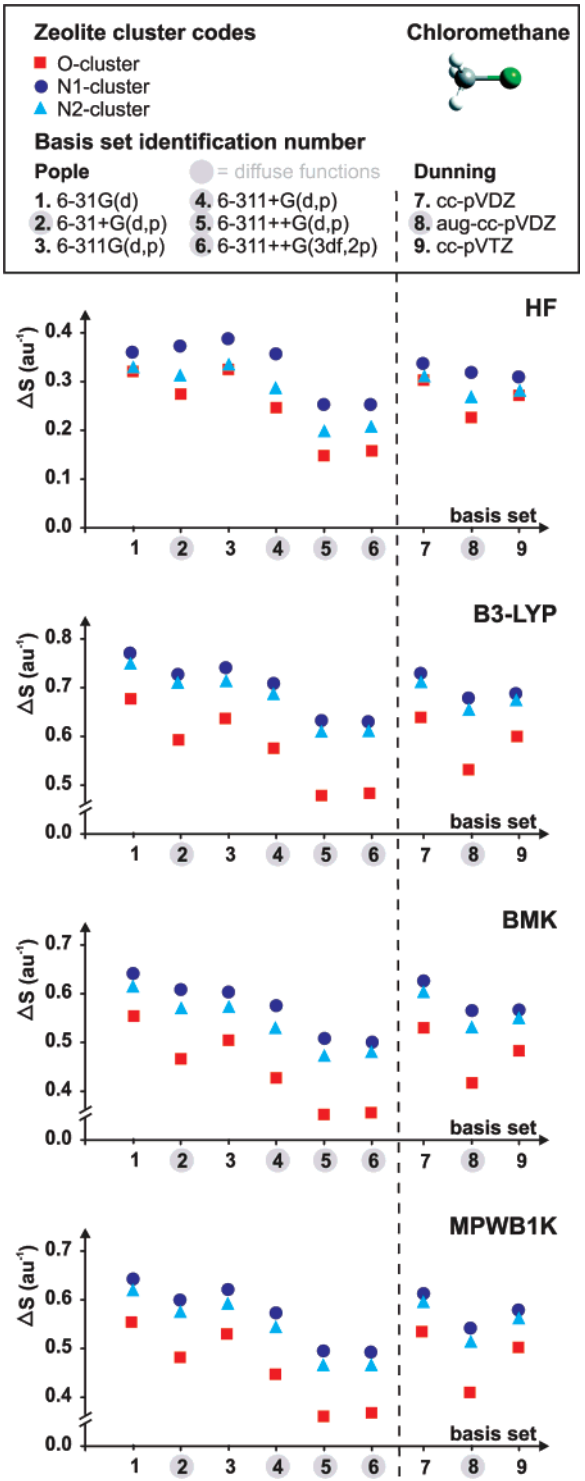

Figure 3. ΔS values for the interactions with chloromethane. Red squares correspond to the O cluster, dark blue circles to the N1 cluster, and light blue triangles to the N2 cluster.

First, we find that the overall qualitative basis set dependence of the various DFT functionals is extremely similar. A striking exception is noticed for the interaction with C_2H_4, where augmentation from the Dunning cc-pVDZ basis set leads to a largely deviating behavior for the MPWB1K functional.

Second, for ethylene the basis set dependence is largest in HF. From a quantitative perspective, the HF values are systematically smaller than the DFT results.

Third, the reactivity sequence $\Delta S(O) < \Delta S(N2) < \Delta S(N1)$ is found throughout, for both ethylene and chloromethane. Only

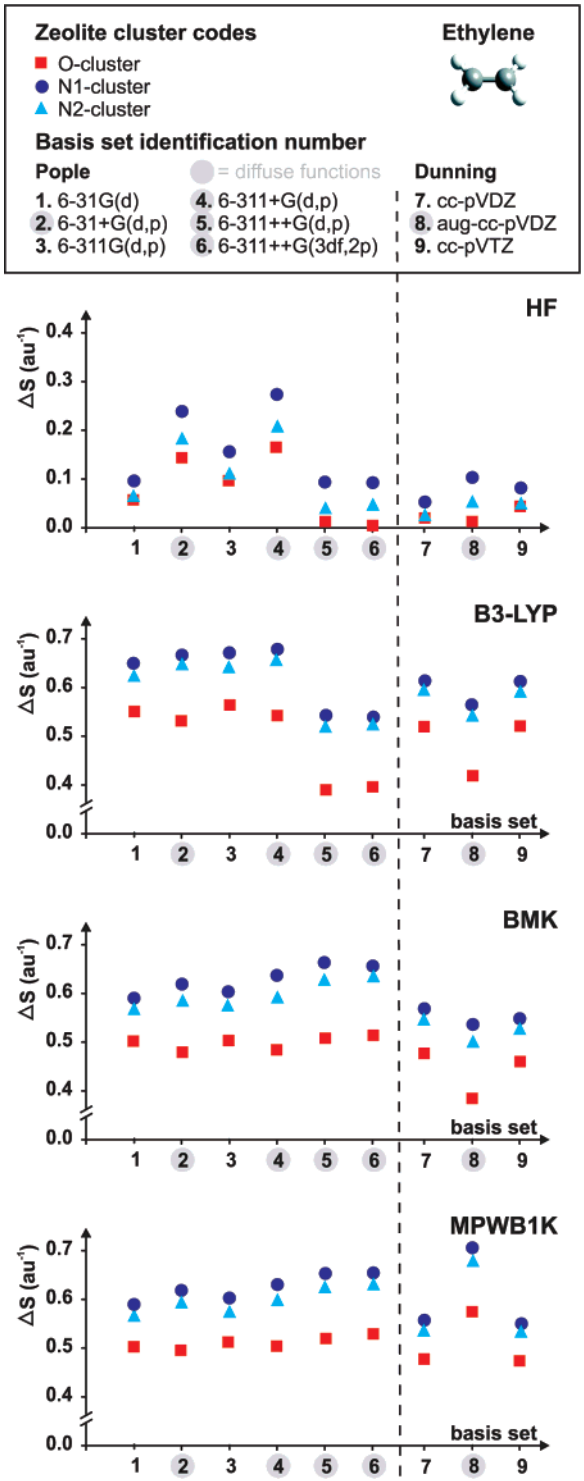

Figure 4. ΔS values for the interactions with ethylene. Red squares correspond to the O cluster, dark blue circles to the N1 cluster, and light blue triangles to the N2 cluster.

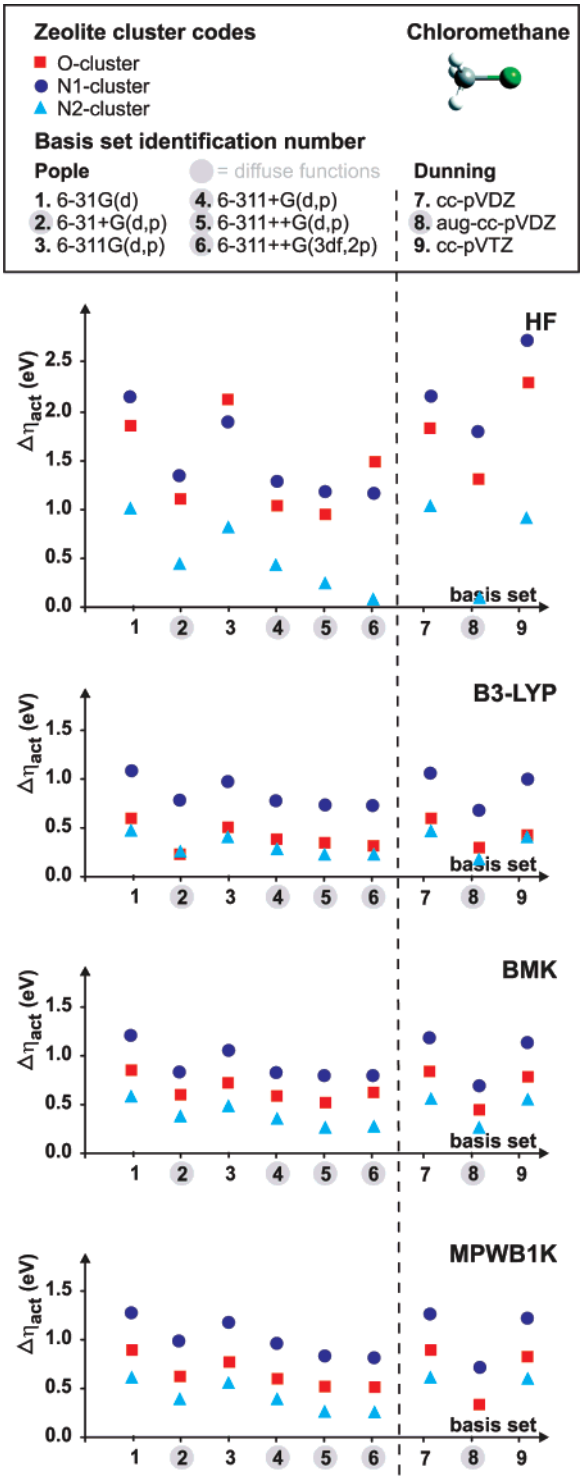

Figure 5. $\Delta\eta_{act}$ values or the interactions with chloromethane. Red squares correspond to the O cluster, dark blue circles to the N1 cluster, and light blue triangles to the N2 cluster.

in the case of ethylene this sequence matches the kinetic results in Table 5. For the studied hard−hard interactions within zeolite catalysis, reactivity sequences based on ΔS values are entirely independent of the computational method used for the calculation of the global reactivity descriptors. This is no guarantee, however, for sequences based on the HSAB principle to coincide with sequences obtained from kinetic data.

4.3.3. Activation Hardnesses. Activation hardnesses were calculated for the interactions between the three zeolite clusters and the probe molecules. Computations on both the optimized structures of the adsorbed reactants and transition structures were performed. Application of the B3-LYP/6-31G(d) level of theory on these systems has already been performed,[28] and an excellent correlation between the $\Delta\eta_{act}$ and ΔE_0 values for all studied reactions was observed. However, does this agreement still hold when the level of theory, used for the single-point energy calculations, is altered? Chloromethane and ethylene (optimized at B3-LYP/6-31G(d)) were again chosen as reference polar and apolar systems, respectively. The results are illustrated in Figures 5 and 6.

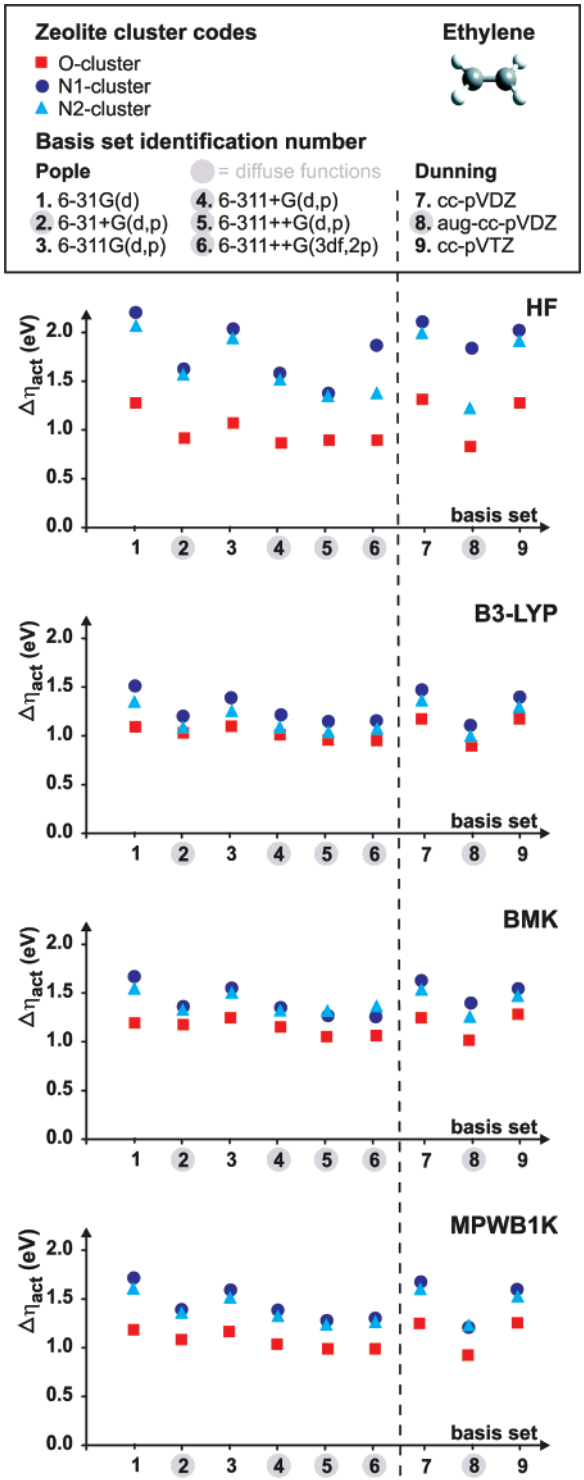

Figure 6. $\Delta\eta_{act}$ values for the interactions with ethylene. Red squares correspond to the O cluster, dark blue circles to the N1 cluster, and light blue triangles to the N2 cluster.

The conclusions about basis set and functional dependence are quite similar to those obtained in the previous section for the ΔS values. The basis set sensitivity of the four methods follows a similar pattern. The HF results show again a larger scattering from the DFT results, the latter which are closer to each other.

For the interaction with chloromethane, the sequence based on reaction barriers is the following: $\Delta E_0(N1) > \Delta E_0(O) > \Delta E_0(N2)$ and this trend is correctly reproduced by all three DFT methods using the $\Delta\eta_{act}$ descriptor. The MPWB1K/aug-cc-pVDZ result for the N2 cluster has been omitted due to spin-contamination in the calculation of the cation. The HF results show occasional deviations from this sequence, more precisely when the 6-311G(d,p) (**3**), 6-311++G(3df,2p) (**6**) basis sets are used. As mentioned earlier, HF performs poorly for the computation of $\Delta\eta_{act}$ values, underlying the importance of including correlation effects for an accurate energy calculation of the adsorbed reactants and transition structures.

For the interaction with ethylene, the correct sequence is different: $\Delta\eta_{act}(N1) > \Delta\eta_{act}(N2) > \Delta\eta_{act}(O)$. Here all levels of theory succeed in reproducing correctly this sequence. Only the BMK functional predicts an occasional reversed sequence between the N1 and N2 clusters, albeit based on very small differences.

5. Conclusions

We have thoroughly assessed the level-of-theory dependence of important molecular properties, such as the ionization potential and electron affinity, as well as global reactivity descriptors, such as the chemical potential and global hardness. This investigation was concentrated on typical interactions within zeolite catalysis between small probe molecules (chloromethane, methanol, ethylene, and propene) and three model zeolite clusters. All calculations were submitted to an extended set of computational methods. First of all, the dependence on electronic structure method was investigated by testing the HF and three DFT methods, in particular B3-LYP, BMK, and MPWB1K. The performance of the latter two hybrid meta-DFT functionals for the computation of reactivity descriptors was hereby addressed for the first time. The basis set dependence on the other hand was also intensively studied, using a broad set of both Pople and Dunning basis sets.

Comparison with available experimental data and high-level post-HF calculations shows that, at least for the small molecules, quantitatively accurate and reliable results can be obtained using any of the aforementioned DFT functionals in conjunction with a basis set of at least double-ζ quality, further augmented with a set of polarization and diffuse functions. The interactions between the oxygen-cluster and the probe molecules are addressed by investigating the global softness differences and activation hardnesses. We generally find similar performance for the three investigated DFT functionals, with the BMK and MPWB1K results particularly close to each other. The HF results, on the other hand, are more scattered and sensitive to the applied basis set.

As the reactivity descriptors are often applied to investigate intermolecular reactivity sequences, we found it crucial to investigate whether these sequences depend on a particular choice of computational method. In this view, three model clusters containing both oxygen and amine bridges were studied in detail. The ordering of the global hardness values is retained, no matter what electronic structure method or basis set is used. The same conclusion holds for the global softness differences, for interactions with both polar and apolar probe molecules. The reactivity ordering, based on activation hardnesses, turns out to show a minor dependence on the level of theory used. Comparison between the DFT functionals demonstrates an extreme similarity between BMK and MPWB1K results, while they both deviate substantially from the B3-LYP results. However, this deviation is only manifested from a quantitative, but not from a qualitative perspective. We gladly report that, for the studied hard−hard interactions, reactivity sequences are mainly independent of DFT functional and/or basis set used. In particular, the previously mentioned necessity to include

diffuse functions is not as strict when focus solely lies on obtaining reliable qualitative reactivity trends. Furthermore, the reactivity sequences obtained using the reactivity descriptors are overall in agreement with sequences based on ab initio reaction energies. An exception is found for the interactions between the oxygen-bridged zeolite cluster and the polar molecules, where the reactivity ordering is not in accordance with the HSAB principle.

Acknowledgment. This work is supported by the Fund for Scientific Research—Flanders (FWO), the Research Board of Ghent University, and the Institute for Science and Technology (I.W.T.).

Supporting Information Available: Global hardness of the purely oxygen-bridged cluster using various levels for the geometry optimization (Figure S1); average softness differences between the purely oxygen-bridged cluster and the probe molecules using various levels for the geometry optimization (Table S1); chemical potential for the probe molecules (Table S2); reaction barriers using various levels for the single-point energies (Table S3); ionization potentials, electron affinities, chemical potentials and global hardnesses for the amine-substituted zeolites N1 (Table S4) and N2 (Table S5). This material is available free of charge via the Internet at http://pubs.acs.org.

References and Notes

(1) Kohn, W.; Becke, A. D.; Parr, R. G. *J. Phys. Chem.* **1996**, *100*, 12974.

(2) Parr, R. G.; Yang, W. *Density-Functional Theory of Atomsand Molecules*; Oxford Science Publications, New York, 1988.

(3) Geerlings, P.; De Proft, F.; Langenaeker, W. *Chem. Rev.* **2003**, *103*, 1793.

(4) Parr, R. G.; Donnelly, R. A.; Levy, M.; Palke, W. E. *J. Chem. Phys.* **1978**, *68*, 3801.

(5) Parr, R. G.; Pearson, R. G. *J. Am. Chem. Soc.* **1983**, *105*, 7512.

(6) Chermette, H. *J. Comput. Chem.* **1999**, *20*, 129.

(7) (a) De, Proft, F.; Martin, J. M. L.; Geerlings, P. *Chem. Phys. Lett.* **1996**, *256*, 400. (b) De Proft, F.; Martin, J. M. L.; Geerlings, P. *Chem. Phys. Lett.* **1996**, *250*, 393. (c) Langenaeker, W.; De Proft, F.; Geerlings, P. *J. Mol. Struct. (THEOCHEM*) **1996**, *362*, 175. (d) Arulmozhiraja, S.; Kolandaivel, P. *Mol. Phys.* **1997**, *90*, 55. (e) Thanikaivelan, P.; Padmanabhan, J.; Subramanian, V.; Ramasami, T. *Theor. Chem. Acc.* **2002**, *107*, 326. (f) Martin, F.; Zipse, H. *J. Comp. Chem.* **2005**, *26*, 97. (g) Cioslowski, J.; Martinov, M.; Mixon, S. T. *J. Phys. Chem.* **1993**, *97*, 10948. (h) Gilardoni F.; Weber, J.; Chermette, H.; Ward, T. R. *J. Phys. Chem. A* **1998**, *102*, 3607.

(8) De Proft, F.; Geerlings, P. *J. Chem. Phys.* **1997**, *106*, 3270.

(9) (a) Jalbout, A. F.; Darwish, A. M.; Alkahby, H. Y. *J. Mol. Struct. (THEOCHEM*) **2002**, *585*, 205. (b) Jalbout, A. F.; Jalbout, F. N.; Alkahby, H. Y. *J. Mol. Struct. (THEOCHEM*) **2001**, *574*, 141.

(10) Chattaraj, P. K.; Schleyer, P. v. R. *J. Am. Chem. Soc.* **1994**, *116*, 1067.

(11) Simons, J.; Jordan, K. D. *Chem. Rev.* **1987**, *87*, 535.

(12) Curtiss, L. A.; Raghavachari, K.; Trucks, G. W.; Pople J. A. *J. Chem. Phys.* **1991**, *94*, 7221.

(13) Curtiss, L. A.; Redfern, P. C.; Raghavachari, K.; Pople J. A. *J. Chem. Phys.* **1998**, *109*, 42.

(14) Rienstra-Kiracofe, J. C.; Tschumper, G. S.; Schaefer, H. F.; Nandi, S.; Ellison, G. B. *Chem. Rev.* **2002**, *102*, 231.

(15) Martin, J. M. L.; de Oliveira, G. *J. Chem. Phys.* **1999**, *111*, 1843.

(16) Parthiban, S.; Martin, J. M. L. *J. Chem. Phys.* **2001**, *114*, 6014.

(17) Boese, A. D.; Oren, M.; Atasoylu, O.; Martin, J. M. L.; Kallay, M.; Gauss, J. *J. Chem. Phys.* **2004**, *120*, 4129.

(18) (a) Shore, H. B.; Rose, J. H.; Zaremba, E. *Phys. Rev. B* **1977**, *15*, 2858. (b) Schwarz, K. *Chem. Phys. Lett.* **1978**, *57*, 605.

(19) Galbraith, J. M.; Schaefer, H. F. *J. Chem. Phys.* **1996**, *105*, 862.

(20) Tozer, D. J.; De Proft, F. *J. Phys. Chem. A* **2005**, *109*, 8923.

(21) Zhao, Y.; Truhlar, D. G. *J. Phys. Chem. A* **2004**, *108*, 6908.

(22) Boese, A. D.; Martin, J. M. L. *J. Chem. Phys.* **2004**, *121*, 3405.

(23) Hemelsoet, K.; Moran, D.; Van Speybroeck, V.; Waroquier, M.; Radom, L. *J. Phys. Chem. A* **2006**, *110*, 8942.

(24) Astala, R.; Auerbach, S. M. *J. Am. Chem. Soc.* **2004**, *126*, 1843.

(25) Lesthaeghe, D.; Van Speybroeck, V.; Waroquier, M. *J. Am. Chem. Soc.* **2004**, *126*, 9162.

(26) Chan, B.; Radom, L. *J. Am. Chem. Soc.* **2006**, *128*, 5322.

(27) Lesthaeghe, D.; Van, Speybroeck, V.; Marin, G. B.; Waroquier, M. *J. Phys. Chem. B* **2005**, *109*, 7952.

(28) Hemelsoet, K.; Lesthaeghe, D.; Van Speybroeck, V.; Waroquier M. *Chem. Phys. Lett.* **2006**, *419*, 10.

(29) Pearson, R. G. *J. Am. Chem. Soc.* **1963**, *85*, 3533.

(30) (a) Chattaraj, P. K.; Lee, H.; Parr, R. G. *J. Am. Chem. Soc.* **1991**, *113*, 1855. (b) Damoun, S.; Van de Woude, G.; Mendez, F.; Geerlings, P. *J. Phys. Chem. A* **1997**, *101*, 886.

(31) (a) Pearson, R. G. *Acc. Chem. Res.* **1993**, *26*, 250. (b) Parr, R. G.; Chattaraj, P. K. *J. Am. Chem. Soc.* **1991**, *113*, 1854. (c) Chattaraj, P. K.; Ayers, P. W. *J. Chem. Phys.* **2005**, *123*, 086101.

(32) Datta, D. *J. Phys. Chem.* **1992**, *96*, 2409.

(33) Zhou, Z.; Parr, R. G. *J. Am. Chem. Soc.* **1990**, *112*, 5720.

(34) Frisch, M. J.; Trucks, G. W.; Schlegel, H. B.; Scuseria, G. E.; Robb, M. A.; Cheeseman, J. R.; Montgomery, J. A., Jr.; Vreven, T.; Kudin, K. N.; Burant, J. C.; Millam, J. M.; Iyengar, S. S.; Tomasi, J.; Barone, V.; Mennucci, B.; Cossi, M.; Scalmani, G.; Rega, N.; Petersson, G. A.; Nakatsuji, H.; Hada, M.; Ehara, M.; Toyota, K.; Fukuda, R.; Hasegawa, J.; Ishida, M.; Nakajima, T.; Honda, Y.; Kitao, O.; Nakai, H.; Klene, M.; Li, X.; Knox, J. E.; Hratchian, H. P.; Cross, J. B.; Bakken, V.; Adamo, C.; Jaramillo, J.; Gomperts, R.; Stratmann, R. E.; Yazyev, O.; Austin, A. J.; Cammi, R.; Pomelli, C.; Ochterski, J. W.; Ayala, P. Y.; Morokuma, K.; Voth, G. A.; Salvador, P.; Dannenberg, J. J.; Zakrzewski, V. G.; Dapprich, S.; Daniels, A. D.; Strain, M. C.; Farkas, O.; Malick, D. K.; Rabuck, A. D.; Raghavachari, K.; Foresman, J. B.; Ortiz, J. V.; Cui, Q.; Baboul, A. G.; Clifford, S.; Cioslowski, J.; Stefanov, B. B.; Liu, G.; Liashenko, A.; Piskorz, P.; Komaromi, I.; Martin, R. L.; Fox, D. J.; Keith, T.; Al-Laham, M. A.; Peng, C. Y.; Nanayakkara, A.; Challacombe, M.; Gill, P. M. W.; Johnson, B.; Chen, W.; Wong, M. W.; Gonzalez, C.; Pople, J. A. *Gaussian 03*, revision B.03; Gaussian, Inc.: Wallingford, CT, 2004.

(35) Sauer, J. *Chem. Rev.* **1989**, *89*, 199.

(36) van Santen, R. A.; Kramer, G. J. *Chem. Rev.* **1995**, *95*, 637.

(37) Becke, A. D. *J. Chem. Phys.* **1993**, *98*, 5648.

(38) Lee, C.; Yang, W. T.; Parr, R. G. *Phys. Rev. B* **1988**, *37*, 785. (b) Miehlich, B.; Savin, A.; Stoll, H.; Preuss H. *Chem. Phys. Lett.* **1989**, *157*, 200.

(39) Zygmunt, S. A.; Mueller, R. M.; Curtiss, L. A.; Iton, L. E. *J. Mol. Struct. (THEOCHEM)* **1998**, *430*, 9.

(40) Dunning, T. H., Jr.; Peterson, K. A.; Woon, D. E. Basis Sets: Correlation Consistent Sets. In *The Encyclopedia of Computational Chemistry*; Schleyer, P. v. R., Ed; John Wiley: Chichester, U.K., 1998.

(41) Frisch, M. J.; Pople, J. A.; Binkley, J. S. *J. Chem. Phys.* **1984**, *80*, 3265 and references therein.

(42) (a) Woon, D. E.; Dunning, T. H. *J. Chem. Phys.* **1993**, *98*, 1358. (b) Kendall, R. A.; Dunning, T. H.; Harrison, R. *J. Chem. Phys.* **1992**, *96*, 6796. (c) Dunning, T. H. *J. Chem. Phys.* **1989**, *90*, 1007. (d) Peterson, K. A.; Woon, D. E.; Dunning, T. H. *J. Chem. Phys.* **1994**, *100*, 7410. (e) Wilson, A. K.; van Mourik, T.; Dunning, T. H., Jr. *J. Mol. Struct. (THEOCHEM)* **1996**, *388*, 339.

(43) (a) Pople, J. A.; Head-Gordon, M.; Raghavachari, K. *J. Chem. Phys.* **1987**, *87*, 5968. (b) Gauss, J.; Cremer, D. *Chem. Phys. Lett.* **1988**, *150*, 280. (c) Salter, E. A.; Trucks, G. W.; Bartlett, R. J. *J. Chem. Phys.* **1989**, *90*, 1752.

(44) (a) Purvis, G. D.; Bartlett, R. J. *J. Chem. Phys.* **1982**, *76*, 1910. (b) Raghavachari, K.; Trucks, G. W.; Pople, J. A.; Head-Gordon, M. *Chem. Phys. Lett.* **1989**, *157*, 479.

(45) Kimura, K.; Katsumata, S.; Achiba, Y.; Yamazaki, T.; Iwata, S. *Ionization energies, Ab initio assignments, and valence electronic structure for 200 molecules in Handbook of HeI Photoelectron Spectra of Fundamental Organic Compounds*; JapanScientific Soc. Press: Tokyo, 1981.

(46) Vorob'ev, A. S.; Furlei, I. I.; Sultanov, A. S.; Khvostenko, V. I.; Leplyanin, G. V.; Derzhinskii, A. R.; Tolstikov, G. A. *Bull. Acad. Sci. USSR, Div. Chem. Sci.* **1989**, *38*, 1388.

(47) Bieri, G.; Asbrink, L. *J. Electron Spectrosc. Relat. Phenom.* **1980**, *20*, 149.

(48) Krause, D. A.; Taylor, J. W.; Fenske, R. F. *J. Am. Chem. Soc.* **1978**, *100*, 718.

(49) Chandra, A. K.; Uchimaru, T.; Sugie, M.; Sekiya, A. *Chem. Phys. Lett.* **2000**, *318*, 69.